Development and Validation of a Wearable Device to Provide Rich Somatosensory Stimulation for Rehabilitation After Sensorimotor Impairment

Mirka Buist, Shahrzad Damercheli, Minh Tat Nhat Truong, Alessio Sanna, Enzo Mastinu, and Max Ortiz-Catalan, *Senior Member, IEEE*

***Abstract*—Training sensory discrimination of the skin has the potential to reduce chronic pain due to sensorimotor impairments and increase sensorimotor function. Currently, there is no such device that can systematically provide rich skin stimulation suitable for a training protocol for individuals with amputation or major sensory impairment. This study describes the development and validation of a non-invasive wearable device meant to repeatedly and safely deliver somatosensory stimulations. The development was guided by a structured design control process to ensure the verifiability and validity of the design outcomes. Two sub-systems were designed: 1) a tactile display for touch and vibration sensations, and 2) a set of bands for sliding, pressure, and strain sensations. The device was designed with a versatile structure that allows for its application on different body parts. We designed a device-paired interactive computer program to enable structured sensory training sessions. Validation was performed with 11 individuals with intact limbs whose upper arm tactile sensitivity was measured over 5 training sessions. Tactile discrimination and perception threshold were measured using the standard 2-point discrimination and Semmes-Weinstein monofilament tests, respectively. The results of the monofilament test showed a significant improvement ($p = 0.011$), but the improvement was not significant for the 2-point discrimination test($p = 0.141$). These promising results confirm the potential of the proposed training to increase the sensory acuity in the upper arms of individuals with intact limbs. Further studies will be conducted to determine how to transfer the findings of this work to improve the pain and/or functional rehabilitation in individuals with sensorimotor impairments.**

***Index Terms*—Functional rehabilitation, plasticity-guided treatment, sensory training, serious games, neurorehabilitation.**

I. Introduction

SENSORIMOTOR impairment is an umbrella term for diseases and injuries related to the body's function to move and/or sense. It has been hypothesized that sensory training, intended as the training of sensory acuity, has the potential to reduce pain due to sensorimotor impairments and potentially increase sensorimotor function [1]. This idea has been explored in the treatment of chronic pain, such as phantom limb pain and complex regional pain syndrome, and stroke rehabilitation [2]. Flor et al. [3] found that both two-point discrimination thresholds and phantom limb pain levels improved after a ten-day sensory training procedure. Similarly, Moseley et al. found similar results in patients with complex regional pain syndrome [4]. Dogru Huzmeli et al. found that sensory training can improve function in stroke patients [5]. However, sensory stimulation in previous work was delivered with manually applied mechanical stimulations or electrical stimulations. Whereas one can find commercially available electrical stimulators for an automated delivery of electric current, the availability of analogous devices to appropriately stimulate all the different mechanoreceptors is limited. The lack of such device poses challenges moving towards a structured sensory training protocol in which the quality, intensity, duration, and location of stimuli is standardized. Such a device would also help to control the interactions between the patient and the stimuli (*i.e.*, interactive games). Automation of the delivery of stimuli is thus desirable to enable replicability of stimuli and interaction. Furthermore, the ideal automated device would optimally stimulate all the different types of skin mechanoreceptors in a physiologically appropriate manner. We emphasis "physiologically appropriate" as this would result in

Manuscript received 14 February 2023; revised 5 April 2023 and 21 April 2023; accepted 23 April 2023. Date of publication 1 May 2023; date of current version 12 July 2023. This work was supported in part by the Promobilia Foundation, in part by the IngaBritt and Arne Lundbergs Foundation, and in part by the Swedish Research Council (Vetenskapsrådet). This paper was recommended by Associate Editor H. Jiang. *(Corresponding author: Max Ortiz-Catalan.)*

This work involved human subjects or animals in its research. Approval of all ethical and experimental procedures and protocols was granted by the governing ethical committee in Sweden under Application No. 2021-03272, and performed in line with the Declaration of Helsinki.

Mirka Buist is with the Center for Bionics and Pain Research, 431 80 Mölndal, Sweden, also with the Bionics Institute, Melbourne, VIC 3002, Australia, and also with the Department of Physiology, Institute of Physiology and Neuroscience, Sahlgrenska Academy, University of Gothenburg, 413 90 Gothenburg, Sweden (e-mail: mirka@chalmers.se).

Shahrzad Damercheli is with the Center for Bionics and Pain Research, 431 80 Mölndal, Sweden, and also with the Department of Electrical Engineering, Chalmers University of Technology, 412 96 Gothenburg, Sweden (e-mail: shadam@chalmers.se).

Minh Tat Nhat Truong is with the Center for Bionics and Pain Research, 431 80 Mölndal, Sweden, and also with the KTH MoveAbility Lab, School of Engineering Sciences, 100 44 Stockholm, Sweden (e-mail: minht@kth.se).

Alessio Sanna is with the Center for Bionics and Pain Research, 431 80 Mölndal, Sweden (e-mail: sannaalessio29@gmail.com).

Enzo Mastinu is with the Center for Bionics and Pain Research, 431 80 Mölndal, Sweden, also with the Department of Electrical Engineering, Chalmers University of Technology, 412 96 Gothenburg, Sweden, and also with the Artificial Hands Area, BioRobotics Institute, Sant'Anna School of Advanced Studies, 56025 Pontedera, Italy (e-mail: enzo.mastinu@santannapisa.it).

Max Ortiz-Catalan is with the Center for Bionics and Pain Research, 431 80 Mölndal, Sweden, also with the Bionics Institute, Melbourne, VIC 3002, Australia, and also with the Department of Electrical Engineering, Chalmers University of Technology, 412 96 Gothenburg, Sweden (e-mail: maxo@chalmers.se).

Color versions of one or more figures in this article are available at https://doi.org/10.1109/TBCAS.2023.3271821.

Digital Object Identifier 10.1109/TBCAS.2023.3271821

TABLE I
SOMATOSENSORY ACTUATORS

Reference	Title	Actuator	Size of actuator
Gallo et. al. [6]	A flexible multimodal tactile display for delivering shape and material information	Micro-sized solenoids and Peltier elements	23x23 mm
Vechev et. al.[7]	TacTiles: Dual-mode low-power electromagnetic actuators for rendering continuous contact and spatial haptic patterns in VR	Micro-sized solenoids	17x17 mm
Carter et. al. [8]	UltraHaptics: Multi-point mid-air haptic feedback for touch surfaces	Ultrasound display	160x200 mm
Uramune et al [9]	HaPouch: A Miniaturized, Soft, and Wearable Haptic Display Device Using a Liquid-to-Gas Phase Change Actuator	Chemically induced actuator	13x13 mm
Sonar and Paik [11]	Soft pneumatic actuator skin with piezoelectric sensors for vibrotactile feedback	Vibration actuators	4x4 mm
Clemente et. al. [12]	Non-Invasive, Temporally Discrete Feedback of Object Contact and Release Improves Grasp Control of Closed-Loop Myoelectric Transradial Prostheses	Vibration actuators	55x42 mm
Bianchi [13]	A fabric-based approach for wearable haptics	Fabric Bands	150x150 mm
Sullivan et. al. [14]	Multi-Sensory Stimuli Improve Distinguishability of Cutaneous Haptic Cues	Vibrators, Fabric Bands, Servo based rocker	100x100 mm
Agharese et. al. [16]	HapWRAP: Soft Growing Wearable Haptic Device	Pneumatic system	230x52.5 mm
Ueda and Ishii [18]	Development of a feedback device of temperature sensation for a myoelectric prosthetic hand by using Peltier element	Peltier elements	50x60 mm
Patel et. al. [19]	Multichannel electrotactile feedback for simultaneous and proportional myoelectric control	Electro tactile stimulation	20x20 mm

afferent discharges as naturally occurring in the peripheral and central nervous systems, and "all the different types" for the versatility to cover the entire repertoire of tactile experiences. For example, it has been hypothesized that a completer and more natural reengagement of neural circuitry related to an impaired body part, would reduce the likelihood of experiencing neuropathic pain [1].

We conducted a literature review to identify state-of-the-art actuators to elicit somatosensations and haptic feedback technologies. The review was performed in August 2020, and updated in March 2023. Search terms used for this review were: "(Haptic OR Tactile) AND Feedback AND Device", "(Haptic OR Tactile) AND Display", and "(Haptic OR Tactile) AND Interface". The review included actuators currently on the market, as well as devices only available within research environments. The review focuses on technologies that have the possibility to be implemented in one wearable device that can be worn in a wide variety of body parts, such as extremities, and torso. Technologies that are only applicable to one specific body part, such as the hands, feet, or head, were excluded. We found a variety of promising mechanisms for haptic feedback, such as micro-magnetic pin actuators, chemically induced actuators, vibration actuators, wrapped bands, pneumatic systems, ultrasound, and Peltier elements. An overview of all mechanisms is presented in Table I , the table includes one example for each mechanism. Each of these methods can induce different sensations, depending on the way they are activated. Micro-sized solenoids [6], [7], ultrasound displays [8], and chemically induced actuators [9], [10], can be used to provide tactile feedback sensed by Merkel's disks. These mechanisms can produce vibrations similar to those generated by Vibration actuators, with the exception of chemically induced actuators, which often exhibit a slow state change [9]. Vibration actuators [11], [12] can be incorporated to stimulate Meisner's and Pacinian Corpuscles. Bands or strings can be used to create sensations of stretch, stroke, or pressure [13], [14], [15], which could also be accomplished by a pneumatic system [16], [17]. Peltier elements can be used for temperature sensation by free nerve endings [18]. Another possibility is to provide electro-tactile stimulation [19], although this is often perceived as unnatural [20], [21], and thus is perceived as less desirable. In principle, several of these methods could be combined to create one wearable haptic device, albeit the challenge seems to lay on the density of actuators one can place side-by-side to reach enough resolution to deliver rich somatosensory stimulation.

In this study, we present a wearable device intended to provide various somatosensations varying from touch, vibrations, sliding, pressure, and strain. The device was designed to be easily adaptable to different users, *e.g.*, different sizes and different residual limbs in case of amputees, as well as different stimulation setups. We verify the functionality of the device in bench tests and consequently validated it with volunteers with intact limbs. Our tests showed that the device can safely provide rich somatosensations and that it has potential to be used clinically as part of treatments for functional rehabilitation and/or alleviation of pain due to sensorimotor impairments.

II. MATERIALS AND METHODS

A. Design Approach

The wearable device was designed according to the waterfall-model following guidelines from the "Design Control Guidance For Medical Device Manufacturers" document of the FDA [22], and following a similar implementation to the one included in the European Medical Device Regulation [23]. The user needs and the consequent technical requirements were set prior to the developmental process. The user needs were established by interviewing potential therapists, patients, and other users. For the sake of conciseness, we report here only the main features

TABLE II
ACTUATOR-RECEPTOR MATRIX

	Ultrasound	Peltier elements	Airflow	Stretch pulleys	**Wrap band**	Kinesthetic device	Vibration actuators	**Ch**emical actuators	**Magnetic actuators**	# #
Meissner's corpuscle - Touch - FA-I	x				**x**			x	**x**	4
Pacinian corpuscle - Vibration - FA-II							x		**x**	2
Ruffini's ending - Skin stretch - SA-II				x	**x**					2
Hair follicle plexus – Sliding and Air - IA			x	x	**x**					3
Merkel's disks - Light touch and small vibration - SA-I	x				**x**		x	x	**x**	5
Free nerve endings - Temperature and pain - IA		x	x							2
Kinesthetics – Joint movement	x			x	**x**	x				4
#	3	1	2	3	**5**	1	2	2	**3**	

of the functional prototype as well as its bench verification and user validation.

The intended device was designed to be able to target as many different sensory receptors as possible. Therefore, mechanisms (i.e., actuators) that could stimulate multiple sensory receptors were given priority, as well as those that can be easily adapted to different body parts. The literature study that was conducted prior to this study resulted in the actuator-receptor matrix in Table II . The actuators presented in the actuator-receptor matrix in Table II, refer to the technologies found in the literature review as presented in Table I. With an effort to simplify and engineer the much-complicated physiological relation between actuators and receptors, Table II visualizes which mechanoreceptors (left column) are predominantly involved in sensing each of the actuators (top row). Such approach was mandatory in order to define priorities within a wide range of available actuators.

In the bottom row of Table II the total number of mechanoreceptors involved in each of the actuators is displayed. Similarly, in the right column of Table II the total number of actuators that can actuate each mechanoreceptor type is displayed. The magnetic actuators could stimulate three mechanoreceptors. The wrap band could stimulate five receptors, of which three were different from the magnetic actuators. Thus, when combining these two mechanisms, six out of seven receptors could be activated. Only free nerve-ending receptors would remain inactivated, responsible for sensations related to temperature and pain. However, at this stage, the activation of free nerve endings was not intended as a priority considering its increased complexity in matters of safety and subjective experience.

Following this rationale, magnetic actuators and wrap bands were deemed as the actuators to be included within the design of the intended device scope of this study. Fig. 1 illustrates how the actuators are linked to each of the mechanoreceptors.

B. The Wearable Somatosensory Device

The design of the wearable device includes the two types of actuators that were selected during the design approach, namely a tactile display and sliding and strain bands, and a versatile enclosure around the actuators. A tactile display was designed using the magnetic actuators, mentioned in Section II-B-1) Tactile displays. Sliding and strain bands were designed using wrap bands, mentioned in Section II-B-2) Sliding and strain bands.

1) Tactile Displays: The tactile display was designed to provide touch and vibration sensations. The tactile display consisted of a 4x4 1-cm resolution grid of solenoid-like actuators. Each point in the grid was an assembly of an electromagnetic coil and a magnetic rod as a core (Fig. 2(a)). By allowing electric current to flow through the coil (*i.e.*, activating the electromagnet) a magnetic field is generated resulting in a force applied on the rod. This force pushes the magnetic rod outwards, resulting in a tactile sensation on the skin. This sensation would predominantly be received by the Merkel's Disks. Vibration could be created by activating and deactivating the electromagnetic coil at a given frequency. A stimulating frequency of about 30 to 50 Hz would be received by the Meisner's Corpuscles. Frequencies above 60 Hz would be received by the Pacinian Corpuscles, with an optimal sensitivity at 250 Hz [24]. The tactile grid design presented here can sustain vibrations up to 250 Hz.

2) Sliding and Strain Bands: Two sets of moveable bands were designed to provide sliding, pressure, and strain sensations. These bands were moved by a system of servomotors whose configuration is illustrated in Fig. 2(c).

The first set consisted of two servomotors, each connected to one end of a rope that could be wrapped around the targeted body part. Activating the two servomotors in the same direction would create a sliding sensation mainly related to the activation of the hair follicle plexus and the Ruffini's Endings due to stretching of the skin. Activating the two servomotors in opposite directions would create a sensation of deep pressure mainly related to the activation of the Pacinian Corpuscles [24]. This set was replicated so to achieve sliding and pressure sensations at both top and bottom sides of the device.

The second set consisted of two symmetrically placed servomotors connected to short ropes. The other side of the ropes was a fixed point to be located on the targeted body part, preferably with its direction aligned with muscle fibers. In Fig. 2(c) these fixed points are located on a small strap that is placed parallel to the main strap of the device. Activating the servomotors would tighten the correspondent rope, which would create a strain force on the skin mainly related to the activation of Ruffini's Endings. It is known that skin stretch can create the illusion of proprioception (*i.e.*, alternating joint configurations [25]), therefore this set of servomotors can be strategically located on a joint in the body so to infer changes (*e.g.*, flexion and extension of the wrist).

3) Versatile Enclosure: All feedback modalities were combined in an agile and flexible sleeve meant to be wearable. The concept sketch of this design is illustrated in Fig. 2(d). Each set of actuators was placed in a case with a surface of 45x45 mm.

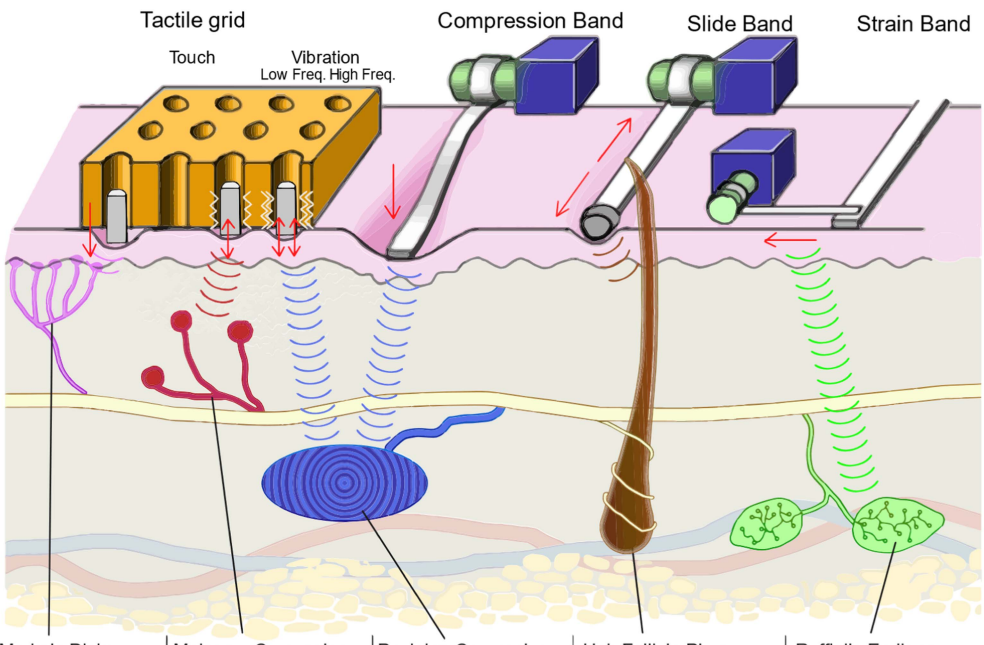

	Merkels Disks	Meisners Corpuscles	Pacinian Corpuscles	Hair Follicle Plexus	Ruffini's Endings
Type	Slow Adapting	Rapid Adapting	Rapid Adapting	Rapid Adapting	Slow Adapting
Response					
Density [/cm2]	High 500	Medium 100	Low 20	Medium 200	Low 10
Fundtion	Light touch and tactile discrimination	Low frequency vibrations and skin motion	High frequency vibrations and deep pressure	Hair movements	Skin Stretch

Fig. 1. Overview of the actuators in the design and a simplified relation with the corresponding predominant mechanoreceptors. Merkel's disks respond to the touch activation of the tactile grid. Meissner's corpuscles respond to low frequency vibrations of the tactile grid. Pacinian corpuscles respond to high frequency vibrations of the tactile grid and activation of the compression band. Hair follicle plexus respond to activation of the slide band. Ruffini's endings respond to activation of the strain band [24].

The cases were covered with a layer of tricot fabric to ensure comfort on all skin-applied parts. The sleeve consisted of a grid where the cases could be placed above and next to each other. The sleeve could be made from columns with 1, 2, or 3 rows above each other. The flexibility in the number of rows (i.e., the length) allowed for the use of patients with different limb and/or stump sizes. Each column of the sleeve was a separate piece. Multiple columns could be connected to create a wide band. Due to the flexible material of the sleeve, the band could be wrapped around the limb. The variable number of columns allowed for different limb circumferences. Similarly, a larger number of columns can allow the device to be placed around other parts of the body such as the chest. The flexible spacers in between the columns of the sleeve allowed for the sleeve to wrap around the limb. Such modular system was ideal for the first prototype which was tested on different users. However, future versions could potentially be custom-designed in different sizes to allow for a more robust device.

C. Device Verification

In order to verify the safety and performance of the device, bench tests were performed, and calculations were done. The calculations focused on ensuring the safety in the event of any potential malfunctions in the device's components. When a servo motor would move un-intentionally the band should not tighten in a painful or damaging manner. The components and assembly of the tactile display were tested before, during, and after the assembly to ensure performance. The continuity of the coil's wire connection was checked using a multimeter. The coils were left to vibrate for at least 5 minutes continuously to test the endurance. The driver boards were also checked visually and with a multimeter. The bands were tested in a similar fashion. In these tests, the focus lay on ensuring that the two-servomotors on each end of the band would rotate at the same speed. These tests were done by sliding the band for 2 seconds in one direction and then 2 seconds in the other direction. In this test the displacement was measured on a fixed point of the band. The tension on the band was visually assessed and had to remain equal over the course of the movement to ensure that the band would not loosen or get too tight. Once the assembly was complete, the full device ran a test-script of 2 hours of various activations to further test the endurance.

The software and firmware were also tested on their performance. These tests focused on adequate command and error handling, correct execution of functions, and endurance. Besides

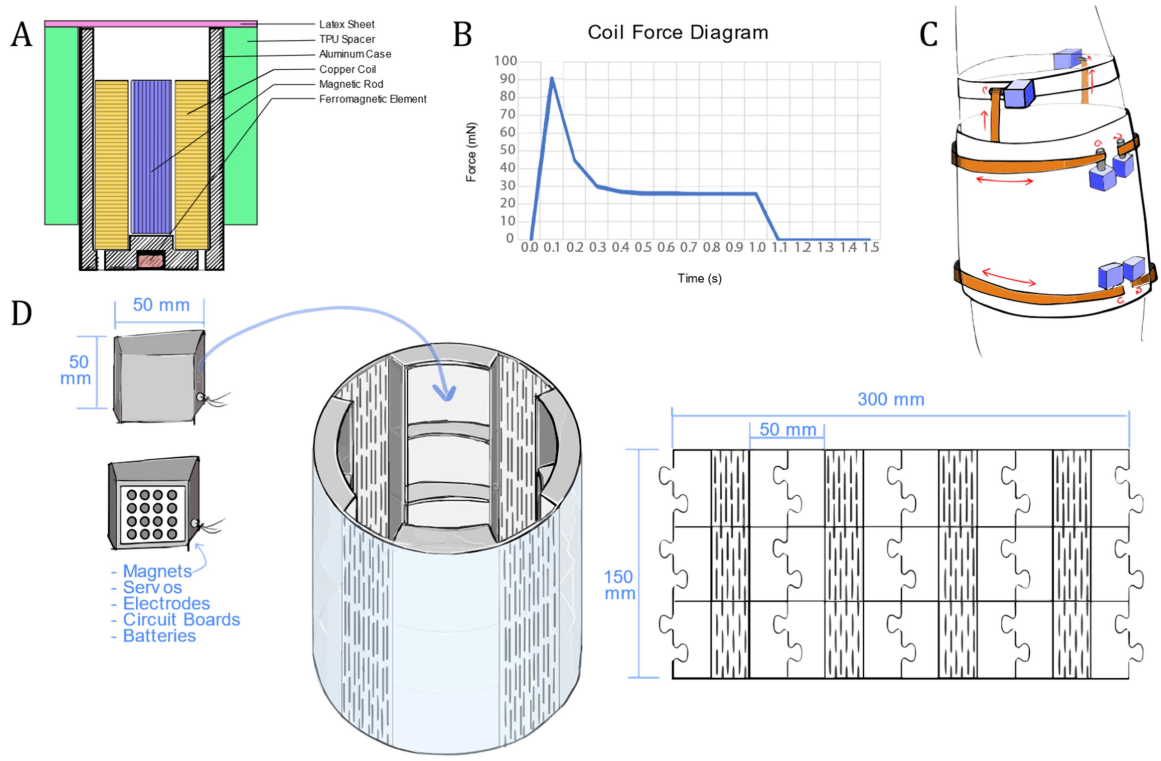

Fig. 2. Design sub-systems. (a) Tactile unit cross section. (b) Coil force diagram. The line shows the force upon activation at T = 0 s and deactivation at T = 1 s. (c) Bands. The two servos on the top are activating the strain bands. The other servos are activating the pressure and sliding bands. (d) Modular case system concept sketch.

test-runs to ensure the functionality was as expected, the delay between software commands and actuator activations was measured. A delay below 250 ms is set as a requirement to ensure the delay below the threshold for humanly perceivable delays [26].

D. Validation With Volunteers With Intact Limbs

The proposed device was validated with individuals with intact limbs. Eleven volunteers with intact limbs volunteers (6 male, 5 female, average age 30.9 (SD±6.8)) were enrolled. All participants signed informed consent prior any this study. The study was approved by the Swedish regional ethical committee in Gothenburg (Dnr:2021-03272).

Such validation meant to demonstrate the feasibility of training tactile sensitivity in non-dominant upper arms. The tactile sensitivity was measured via 1) conventional tactile assessments, and 2) scores of the sensory exercises. The assessments were taken before and after the training sessions.

A total of five sensory training sessions were performed by each participant. Before the first and after the final session the static two-point discrimination (2PD) and the Semmes-Weinstein monofilament tests (MFT) were performed to measure the influence of the sensory training on the tactile detection thresholds. The timeline of the study can be seen in Fig. 3. The wearable training device was placed over the same patch of skin during each training session. Similarly, six related areas of the skin were selected for the tactile sensitivity assessments:

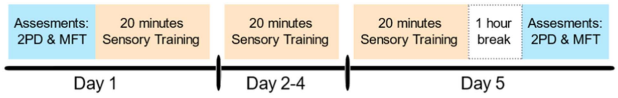

Fig. 3. Timeline of the validation experiment. The experiment consists of 5 consecutive days of 20 minutes effective training time. The assessments (2PD and MFT) were done before the first, and (at least) 1 hour after the last training session.

four points under the tactile displays (i.e., trained skin area), and two points outside (i.e., untrained skin area or control). All points were within 1 cm from the midline of the training device. Removable skin marks and pictures were used to precisely reposition the device between sessions, as well as to perform the assessments on the same points.

1) Tactile Assessments: **2-point Discrimination test**. The 2PD test was meant to find the minimum distance that can be perceived between two points. The test required an applied part, namely the discriminator, with two prongs distributed at predefined distances of 60, 55, 50, 45, 40, 35, 30, 25, 20, 15, 14, 13, 12, 11, 10, 9, 8, 7, 6, 5, 4, 3, 2 mm. For the distances of 25 cm and below we used the 'Dellon Disk-Criminator' and for all the larger distances we used a 3D printed probe similar to the 'Dellon Disk-Criminator' that we designed ourselves. The latter was used to avoid time-loss and inaccuracies by adjusting a pair of compasses or calliper for every distance. During the test, the discriminator was applied longitudinally and perpendicularly to the selected skin areas with one or two prongs, ten times

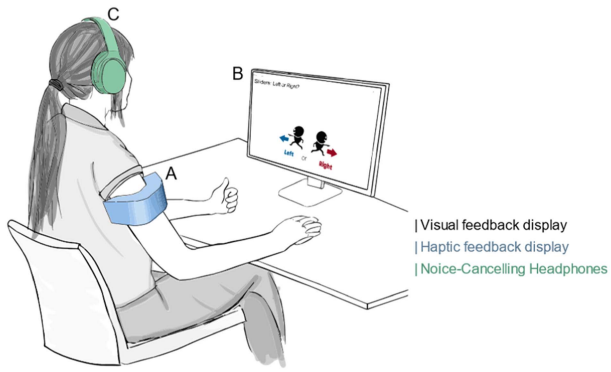

Fig. 4. Schematic illustration of the setup used for the validation experiment. The wearable training device (a) was placed on the upper arm of the non-dominant arm of the participant. A user-interface (b) provides instructions for the training. Noise-canceling headphones (c) with a white-noise soundtrack were used to isolate the user from the sounds of the actuators.

Fig. 5. Wearable somatosensory device for training tactile sensitivity.

randomly. The application was kept as uniform as possible for about 1 second, with a pressure just sufficient for skin blanching. Starting from the largest, each distance was applied 10 times in random order (one/two prongs), and 7 correct answers were needed to proceed to the next lower distance. [27]

Monofilament test: The MFT was meant to find the minimum force that can be perceived. The test required a set of applied parts (i.e., the monofilaments) ordered by different sizes and equivalent applied force: 0.6, 0.4, 0.16, 0.04, 0.02 g. During the test, the filaments were applied for about 2 seconds perpendicularly to the skin targeting a bend of approximately 1 cm. Starting from the smallest, each filament was applied at most 3 times randomly in each of the six selected areas. The participant was asked to report the sensation, if any, in combination with the corresponding location. One correct identification of sensation and location was enough to verify the detection threshold. Moving to the next larger force if the sensation was not correctly identified at a certain location. [28]

2) Training Sessions: A training session was designed to promote the development of tactile sensory acuity by challenging the participants in sensory discrimination tasks using serious games.

Each training session lasted about 30 minutes. In each session, participants were sat in a comfortable position in front of a screen where the training tasks were running. Instructions about the tasks were shown on the screen and explained by the experimenter when needed. Result scores were automatically calculated and plotted out at the end of each task. Participants were isolated from the sound of the actuators by listening to loud-enough white noise via noise-canceling headphones. This setup is shown in Fig. 4.The training tasks comprised of recognizing and discriminating different somatosensations provided by the wearable device in combination with screen instructions. For example, executing sensory discrimination tasks like "which of the following vibrations has a higher frequency?", or "are the bands sliding or applying pressure?", or "in which direction are they moving?", or "which pattern is now on the tactile display?". The training software comprised of three different sensory training modalities. The first modality was a set of multiple-choice questions where the participant had to find the initial given sensation between the multiple-choice answers. The second modality was a Memory game where the participant was asked to match pairs of two similar sensations between a set of 8 to 12 different options. The last modality was a discrimination task where the participant had to identify if the sensations felt with the tactile display were similar or different on each of the displays. The given sensations were, for example, vibrations at different frequencies, movement directions, or various shapes or locations on the tactile grid.

These tasks were then proposed as single events iterated multiple times or as part of more complex games, like the Memory game where discrimination and recognition were tested together. Finally, these tasks were grouped and ordered by difficulty (i.e., easy, medium, and hard). The experimenter supervised all training sessions and decided which difficulty level to perform based on previous scores (i.e., at least 80% to advance to the next level), trying always to keep the participant at an adequate engagement [29]. All training software was written in Matlab (Mathworks, USA).

E. Statistical Analysis

Datasets were analyzed using built-in statistics functions of MATLAB 2018b. The one-sample Kolmogorov-Smirnov test ($p > 0.7$) was used to verify the normality of the distributions of the datasets. Since the datasets exhibited non-normal distributions, the Wilcoxon signed-rank test was used for the paired comparisons of tactile sensitivity assessments. The test compared the data from before with after the training sessions. The signed-rank test could be used because the data was paired, as each testing cite was tested before and after.

III. Results

A. Specifications of the Device

The wearable device was developed according to the previously described design. The wearable device, shown in Fig. 5, included a central unit for control electronics, two tactile displays, two sliding bands, and two strain bands. The specifications of each component can be seen in Table III . The control

TABLE III
DEVICE SPECIFICATIONS

Tactile unit specifications	
Coil outer diameter	5.5 mm
Coil inner diameter	3.5 mm
Coil length	9.5 mm
Inductance	838.7 µH
Steady current draw	0.050 A
Peak current	0.150 A
Magnet diameter	3mm
Magnet length	8mm
Magnet grade	N42
Impact force	90 mN
Sliding bands specifications	
Servo current	0.2 A
Torque	2.0 kgf-cm (0.20 N·m)
Rope length	20 cm
Rope width	0.3 cm
Maximum force	3.9 N/cm2
Maximum speed	0.05 m/s
Compression bands specifications	
Servo current	0.35 A
Torque	2.5 kgf-cm (0.25 N·m)

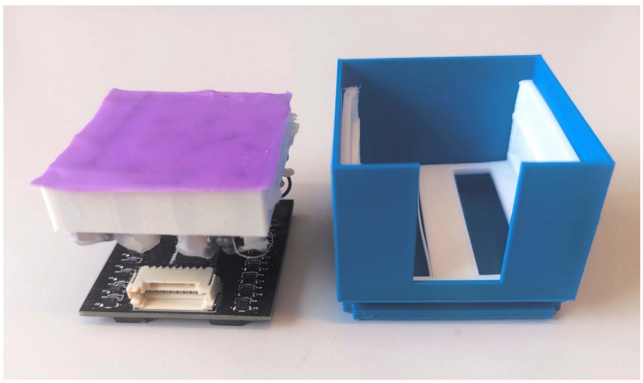

Fig. 6. Tactile display outside of its 3D printed case.

electronics were based on an ARM Cortex-M4 microcontroller USB-connected to a computer, while the actuators were powered via external power supply certified for medical use (GSM25E05, Mean Well, Taiwan).

1) Tactile Displays: The tactile displays consist of 16 tactile units in a grid of 4 by 4 points, which can be seen in Fig. 6. Each tactile unit consisted of a coil with 0.1 mm thick copper wire, with an inner diameter of 3.5 mm, an outer diameter of 5.5 mm, and a height of 9.3 mm. The coils had a total of 750 windings per piece. The magnetic rod in the center of the coil had a diameter of 3 mm and was 8 mm long. The rods had a magnetic rating of grade N42. The coils were surrounded by an aluminum case to shield the magnetic field. The tactile units were positioned in a grid of solid 3D printed plastic material. This di-magnetic material reduced the interference of the coils and magnets on each other. Moreover, the tactile units were disposed in the grid with alternated supplies polarity, so to further reduce interferences. The center distance between each of the tactile points was 11.0 mm. This distance was set below the two-point discrimination functionalities of limbs (the lowest threshold is 21.5 mm at the medial lower arm [30]). At the same time, the distance was large enough to ensure limited interference.

The electronic circuit driving each point in the grid was designed to reduce power consumption. This circuit consisted of a transistor in common emitter configuration and a large capacitor placed in series between the coil and the transistor collector. When the transistor is activated, the charge of the capacitor would allow an immediate high current (0.150 A) to flow through the coil, generating enough field to move the rod. Then, as soon as the capacitor is fully charged the current would settle on a lower steady value (0.050 A) determined by a resistor placed in parallel to the capacitor. This circuit allowed a reduction of power consumption by 67% and a maximum impact force of each tactile point of 90 mN when activated with 5 V (Fig. 2(b)).

2) Sliding Bands: The slide and pressure band used continuous servomotors and two spools to allow the band to wind around them. A knot was added onto the slide band so to indicate a specific location on the slider axis. The servomotors had dimensions of 50.4 × 37.2 × 20 mm and weighed 40 g. The spool had a radius of 0.6 cm. The servomotors required a current of 0.2 A at 5.0 V when operated, producing a torque of 2.0 kgf-cm (0.20 N·m). Having two servos at opposite sides resulted in a maximum force of 2.4 kgf (23.5N). The rope applied pressure over its whole surface of roughly 6 cm^2 (20 cm in length and 0.3 cm in width). The resulting maximum force was about 3.9 N/cm^2. This is far below the average pain pressure threshold in extremities, which varies between 100 and 200 N/cm^2 depending on the location [31]. This implies that in case of erroneous activation of both servos, the band could not do any harm to the user. This configuration resulted in a sliding speed between 0 and 0.05 m/s. The total length of the rope was decided as at least two times the circumference of the targeted limb to ensure that the knot could travel fully around the limb. The case around the servo and spool was designed to ensure that the rope was neatly winded on the spool without unraveling.

For the compression band, micro-sized position-controlled servomotors were used. The servomotors had dimensions of 2.5 × 2.5 × 1.5 cm and weighed less than 10 grams. The servomotors required a current of 0.35 A at 5.0 V when operated, producing a torque of 2.5 kgf-cm (0.25 N·m).

B. Verification of the Device

The technical requirements regarding device safety and comfort were verified by looking at the rationale of the above-described design. None of the aforementioned actuators can reach an activation force that can be considered hazardous for the user. The case was designed in such a way that the parts in contact with the skin were comfortable and not hazardous. The agile design of the case allowed for wide variability in sizes. The minimum height and inner diameter are 5 centimeters and there is no upper limit in size. Therefore nearly anyone could wear the device on an upper or lower limb, or even around the torso. The device was far within the ergonomic weight limitations of 2.2 Kg [32]. The device was found easy to wear using only one hand, as it can be worn as a sleeve.

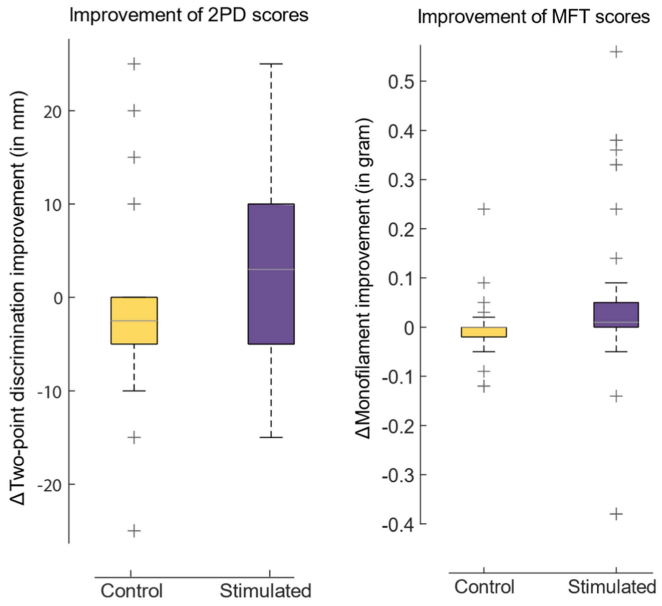

Fig. 7. Results from 2-points-discrimination, or 2PD, test (left) and monofilament, or MFT, test (right). The results are presented as improvement between before and after the training (i.e., difference between day 1 and day 5). $*$ = ($p < 0.05$).

TABLE IV
IMPROVEMENT FROM 2-POINTS-DISCRIMINATION, OR 2PD, TEST AND MONOFILAMENT, OR MFT TEST, OR MFT. THE RESULTS ARE CALCULATED AS IMPROVEMENT BETWEEN BEFORE AND AFTER THE TRAINING (I.E., DIFFERENCE BETWEEN DAY 1 AND DAY 5)

		Mean	IQR	Mdn	*p*
2PD	Control	-1.1363	5	-2.5	0.6203
	Stimulated	2.5454	15	3	0.1405
MFT	Control	-0.0045	0.02	0	0.4460
	Stimulated	0.0513	0.05	0.01	0.0107

The technical requirements regarding device functionalities were verified by bench tests meant to put the whole assembly under intense stress and unveil issues within the electronic and mechanic parts. Such bench tests did not result in any major issues. The calibration of the servomotors suffered minor deviations after hours of continuous activations. This indicated that a recalibration might be needed after intense use.

The delay between software commands and actuator activations was measured to be 261.6 ms on average (SD$\pm$4.8 ms), slightly above the commonly used threshold of 250 ms for humanly perceivable delays [26].

C. Validation With Volunteers With Intact Limbs

The results from 2PD and MFT are shown in Fig. 7 and Table IV presented as improvement between before and after the training (i.e., difference between day 1 and day 5). As expected, the training sessions had little to no effect on the tactile sensitivity of the control areas (i.e., untrained skin patches) for both 2-point and force discrimination ($p = 0.620$ and $p = 0.446$, respectively). When it comes to the stimulated skin patches, a trend of improvement was found for both 2-point and force discriminations. However, this trend was found statistically significant only for the force discrimination ($p = 0.011$) and not significant for the 2-point discrimination ($p = 0.141$). It is good to note that the improvements have high subject-dependent variability. Outliers are present both below the lower inner fence and above the upper inner fence, indicating mild outliers on both sides [33].

The scores from the training tasks and games overall improved for all participants. All participants advanced to more difficult levels, and the majority settled on medium and hard levels. Usually, participants passed the easy level after one or two sessions. The medium level was used the most on average from day 2 to day 4. Seven participants reached the hard level at least twice during all sessions, and the other four at least once.

IV. DISCUSSION

In this study, we presented the design, verification, and validation of a wearable device capable of providing different types of somatosensory stimulation on the skin. The bench verification proved that the device can safely and systematically generate the intended stimuli over long-term repeated activations. All actuators were fully functional after intense testing, and the verification process confirmed that all technical requirements were met. The chosen actuators were capable of stimulating the major mechanoreceptors of the human skin as intended.

As previously reported, stimuli temporal inconsistencies above 250 ms might reduce the user's performance [26]. Our measured stimuli delay was slightly above this threshold. However, the nature of the currently implemented training tasks was not focused on real-time feedback. Therefore the delay was deemed acceptable for this implementation. Nevertheless, it is highly desirable to reduce such delay in future implementations. The delay is due to the implemented communication protocol, specifically to the command-reply time of the device. Such deviation was deemed acceptable at this stage, where we gave priority to receive informative feedback from the device for every given command, so to properly monitor all activations. Future optimization can definitely reduce such reply time or even leave the reply optional for the most time-critical commands.

The tactile display's resolution is still limited. Currently, the intensity of stimulation is fixed and depends on the supply voltage. The impact force produced with 5 V supply was comparable with other work in literature [34], [35] and sufficient to be perceived by all participants with intact limbs. However, this might not successfully translate to compromised anatomical situations such as amputations, scar tissue, or excessive fat tissue. Lastly, the current display has 4x4 actuators, which can be easily expanded to larger matrices. Importantly, the resolution of stimulation is below the standard perception threshold for 2-point discrimination on arms and legs, thus providing enough stimulation resolution.

Despite the promising preliminary results obtained in this study, further improvements can make the device more robust to mechanical breakage, and thus more reliable over time. In addition, a second iterative design approach will try to pursue unsupervised home-use and single-handed user-friendliness.

The validation proved that this device has promising potential to be used for training tactile acuity. The MFT assessment showed significant improvements. The 2PD assessment did

not show a significant improvement. Limitations on statistical significance for the 2PD test could be attributed to the limited training regime, composed of only five training days of 30 minutes each. This protocol is considerably more compact than conventional protocols for functional and pain rehabilitation [36], [37], [38]. Other studies focusing on sensory training have found improvement in the 2PD after training [3], [39], [40], however, these studies were either more extensive [39] or they used the same stimulation device for both training and 2PD measurement [3], [40]. The latter logically aids the improvement as the participant becomes more familiar with the type of stimulation (learning effects). We aim to conduct further studies on patients with sensorimotor impairments where changes in sensory acuity will be evaluated.

Following the various studies as cited in the introduction to treat phantom limb pain and complex regional pain syndrome [3], [4], as well as in stroke rehabilitation [5], we believe the presented device is a potentially useful tool in rehabilitation and pain treatment [1]. The different actuators for somatosensory stimulation can be mapped to different serious gaming features by software. Serious gaming has been investigated for decades as a valid tool for rehabilitation as well as prosthetic use training [41]. The different types of feedback could be mapped to different in-game events or variables. The mapping can be done in numerous ways, such as sliding the bands to left and right to represent the turns of a car in a racing game or the paddle in the breakout game; activating the bands to create proprioceptive illusion to mimic particular joint motions; activating the tactile grid to represent the particular patterns like the pixels of a Tetris game; activating vibration and pressure to notify the user of sudden events like collecting an item or crashing a car. Similarly, a custom training program could be developed to train discrimination of sensations between different body parts, *e.g.*, the affected limb vs contralateral limb. In future work, this device will be used to explore novel rehabilitation protocols for individuals with sensorimotor impairments [1]. This includes clinical studies relating to the reduction of neuropathic pain [38], and improvement of function after stroke or nerve injuries. Our intention in designing a device that could stimulate all mechanoreceptors was precisely to enable research on the effect of sensory training on the treatment of neuropathic pain and functional rehabilitation.

V. Conclusion

The objective of this study was to design and test a wearable device capable of providing rich somatosensory stimulation to be ultimately used for a structured intervention for pain and/or functional rehabilitation. This objective was achieved by combining tactile displays of small electromagnets with sets of moving bands. The 1-cm resolution of the 4x4 tactile displays could create touch sensations on the skin as well as vibrate up to 250 Hz. The moving bands could generate sliding, pressure, and stretching sensations. All actuators were combined in an agile, wearable, sleeve system that easily allows for sizes and configuration adjustments. The device was successfully verified proving reliability and safety suitable for clinical use. Moreover, the device showed promising potential for training tactile acuity. Further studies will be conducted to verify if our current results transfer to individuals with sensorimotor impairment.

Acknowledgment

The study was approved by the Swedish regional ethical committee in Gothenburg (Dnr: 2021-03272). The authors have filed a patent related to the technology described in this article. The authors would like to thank all volunteers who took part in this study.

References

[1] M. Ortiz-Catalan, "The stochastic entanglement and phantom motor execution hypotheses: A theoretical framework for the origin and treatment of Phantom limb pain," *Front. Neurol.*, vol. 9, pp. 1–16, 2018, doi: 10.3389/fneur.2018.00748.

[2] A. Graham et al., "Sensory discrimination training for adults with chronic musculoskeletal pain: A systematic review," *Physiotherapy Theory Pract.*, vol. 38, no. 9, pp. 1107–1125, 2022, doi: 10.1080/09593985.2020.1830455.

[3] H. Flor, C. Denke, M. Schaefer, and S. Grüsser, "Effect of sensory discrimination training on cortical reorganisation and phantom limb pain," *Lancet*, vol. 357, pp. 1763–1764, 2001.

[4] G. L. Moseley, N. M. Zalucki, and K. Wiech, "Tactile discrimination, but not tactile stimulation alone, reduces chronic limb pain," *Pain*, vol. 137, no. 3, pp. 600–608, 2008, doi: 10.1016/j.pain.2007.10.021.

[5] E. Dogru Huzmeli, S. A. Yildirim, and M. Kilinc, "Effect of sensory training of the posterior thigh on trunk control and upper extremity functions in stroke patients," *Neurological Sci.*, vol. 38, no. 4, pp. 651–657, 2017, doi: 10.1007/s10072-017-2822-z.

[6] S. Gallo, C. Son, H. J. Lee, H. Bleuler, and I. J. Cho, "A flexible multimodal tactile display for delivering shape and material information," *Sensors Actuators, A Phys.*, vol. 236, pp. 180–189, 2015, doi: 10.1016/j.sna.2015.10.048.

[7] V. Vechev, J. Zarate, D. Lindlbauer, R. Hinchet, H. Shea, and O. Hilliges, "TacTiles: Dual-mode low-power electromagnetic actuators for rendering continuous contact and spatial haptic patterns in VR," in *Proc. IEEE 26th Conf. Virtual Real. 3D User Interfaces*, 2019, pp. 312–320, doi: 10.1109/VR.2019.8797921.

[8] T. Carter, S. A. Seah, B. Long, B. Drinkwater, and S. Subramanian, "UltraHaptics: Multi-point mid-air haptic feedback for touch surfaces," in *Proc. 26th Annu. ACM Symp. User Interface Softw. Technol.*, 2013, pp. 505–514, doi: 10.1145/2501988.2502018.

[9] R. Uramune, H. Ishizuka, T. Hiraki, Y. Kawahara, S. Ikeda, and O. Oshiro, "HaPouch: A miniaturized, soft, and wearable haptic display device using a liquid-to-gas phase change actuator," *IEEE Access*, vol. 10, pp. 16830–16842, 2022, doi: 10.1109/ACCESS.2022.3141385.

[10] J. Ma et al., "A haptic feedback actuator suitable for the soft wearable device," *Appl. Sci.*, vol. 10, no. 24, pp. 1–13, 2020, doi: 10.3390/app10248827.

[11] H. A. Sonar and J. Paik, "Soft pneumatic actuator skin with piezoelectric sensors for vibrotactile feedback," *Front. Robot. AI*, vol. 2, pp. 1–11, 2016, doi: 10.3389/frobt.2015.00038.

[12] F. Clemente, M. D'Alonzo, M. Controzzi, B. B. Edin, and C. Cipriani, "Non-invasive, temporally discrete feedback of object contact and release improves grasp control of closed-loop myoelectric transradial prostheses," *IEEE Trans. Neural Syst. Rehabil. Eng.*, vol. 24, no. 12, pp. 1314–1322, Dec. 2016, doi: 10.1109/TNSRE.2015.2500586.

[13] M. Bianchi, "A fabric-based approach for wearable haptics," *Electronics*, vol. 5, no. 3, pp. 1–14, 2016, doi: 10.3390/electronics5030044.

[14] J. L. Sullivan et al., "Multi-sensory stimuli improve distinguishability of cutaneous haptic cues," *IEEE Trans. Haptics*, vol. 13, no. 2, pp. 286–297, Apr.–Jun. 2020, doi: 10.1109/TOH.2019.2922901.

[15] S. Casini, M. Morvidoni, M. Bianchi, M. Catalano, G. Grioli, and A. Bicchi, "Design and realization of the CUFF - Clenching upper-limb force feedback wearable device for distributed mechano-tactile stimulation of normal and tangential skin forces," in *Proc. IEEE Int. Conf. Intell. Robot. Syst.*, 2015, pp. 1186–1193, doi: 10.1109/IROS.2015.7353520.

[16] N. Agharese et al., "HapWRAP: Soft growing wearable haptic device," in *Proc. IEEE Int. Conf. Robot. Automat.*, 2018, pp. 5466–5472, doi: 10.1109/ICRA.2018.8460891.
[17] K. Y. Choi, N. Elhaouij, J. Lee, R. W. Picard, and H. Ishii, "Design and evaluation of a clippable and personalizable pneumatic-haptic feedback device for breathing guidance," *Proc. ACM Interactive, Mobile, Wearable Ubiquitous Technol.*, vol. 6, no. 1, pp. 1–36, 2022, doi: 10.1145/3517234.
[18] Y. Ueda and C. Ishii, "Development of a feedback device of temperature sensation for a myoelectric prosthetic hand by using Peltier element," in *Proc. Int. Conf. Adv. Mechatron. Syst.*, 2016, pp. 488–493, doi: 10.1109/ICAMechS.2016.7813497.
[19] G. K. Patel, S. Dosen, C. Castellini, and D. Farina, "Multichannel electrotactile feedback for simultaneous and proportional myoelectric control," *J. Neural Eng.*, vol. 13, no. 5, 2016, Art. no. 056015, doi: 10.1088/1741-2560/13/5/056015.
[20] M. Ortiz-Catalan, J. Wessberg, E. Mastinu, A. Naber, and R. Branemark, "Patterned stimulation of peripheral nerves produces natural sensations with regards to location but not quality," *IEEE Trans. Med. Robot. Bionics*, vol. 1, no. 3, pp. 199–203, Aug. 2019, doi: 10.1109/TMRB.2019.2931758.
[21] E. Mastinu et al., "Neural feedback strategies to improve grasping coordination in neuromusculoskeletal prostheses," *Sci. Rep.*, vol. 10, no. 1, pp. 1–14, 2020, doi: 10.1038/s41598-020-67985-5.
[22] Food and Drug Administration Center for Devices and Radiological Health, "Design control guidance for medical device manufacturers," p. 3, 1997. [Online]. Available: https://www.fda.gov/media/116573/download
[23] Official Journal of the European Union, "Regulation (EU) 2017/745 of the european parliament and of the council," 2017. [Online]. Available: https://eur-lex.europa.eu/legal-content/EN/TXT/HTML/?uri=CELEX:32017R0745
[24] D. Purves et al., *Neuroscience*, 3rd ed. Sunderland, MA, USA: Sinauer Associates, 2004.
[25] B. B. Edin, "Strain-sensitive mechanoreceptors in the human skin provide kinaesthetic information," in *Somesthesis and the Neurobiology of the Somatosensory Cortex*, O. Franzén, R. Johansson, and L. Terenius, Eds. Cambridge, MA, USA: Birkhaüser, 1996, pp. 283–294.
[26] T. Waltemate et al., "The impact of latency on perceptual judgments and motor performance in closed-loop interaction in virtual reality," in *Proc. ACM Symp. Virtual Real. Softw. Technol.*, 2016, pp. 27–35, doi: 10.1145/2993369.2993381.
[27] E. Moberg, "Two-point discrimination test. A valuable part of hand surgical rehabilitation, e.g. in tetraplegia," *J. Rehabil. Med.*, vol. 22, no. 3. pp. 127–134, 1990.
[28] S. Weinstein, "Fifty years of somatosensory research: From the Semmes-Weinstein monofilaments to the weinstein enhanced sensory test," *J. Hand Ther.*, vol. 6, no. 1, pp. 11–22, 1993, doi: 10.1016/S0894-1130(12)80176-1.
[29] E. D. J. Ramos Muñoz et al., "Using large-scale sensor data to test factors predictive of perseverance in home movement rehabilitation: Optimal challenge and steady engagement," *Front. Neurol.*, vol. 13, 2022, Art. no. 1281, doi: 10.3389/fneur.2022.896298.
[30] K. Shibin and A. J. Samuel, "The discrimination of two-point touch sense for the upper extremity in Indian adults," *Int. J. Health Rehabil. Sci.*, vol. 2, no. 1, pp. 38–43, 2013. [Online]. Available: https://www.ijhrs.org/?mno=33496
[31] M. Melia et al., "Pressure pain thresholds: Subject factors and the meaning of peak pressures," *Eur. J. Pain (United Kingdom)*, vol. 23, no. 1, pp. 167–182, 2019, doi: 10.1002/ejp.1298.
[32] E. B. Weston, A. M. Aurand, J. S. Dufour, G. G. Knapik, and W. S. Marras, "One versus two-handed lifting and lowering: Lumbar spine loads and recommended one-handed limits protecting the lower back," *Ergonomics*, vol. 63, no. 4, pp. 505–521, 2020, doi: 10.1080/00140139.2020.1727023.
[33] "NIST/SEMATECH e-Handbook of statistical methods," doi: 10.18434/M32189.
[34] F. Pece et al., "MagTics: Flexible and thin form factor magnetic actuators for dynamic and wearable haptic feedback," in *Proc. 30th Annu. ACM Symp. User Interface Softw. Technol.*, 2017, pp. 143–154, doi: 10.1145/3126594.3126609.
[35] X. Yu et al., "Skin-integrated wireless haptic interfaces for virtual and augmented reality," *Nature*, vol. 575, no. 7783, pp. 473–479, 2019, doi: 10.1038/s41586-019-1687-0.
[36] M. Ortiz-Catalan et al., "Phantom motor execution facilitated by machine learning and augmented reality as treatment for phantom limb pain: A single group, clinical trial in patients with chronic intractable phantom limb pain," *Lancet*, vol. 388, no. 10062, pp. 2885–2894, 2016, doi: 10.1016/S0140-6736(16)31598-7.
[37] E. Lendaro et al., "Phantom motor execution as a treatment for phantom limb pain: Protocol of an international, double-blind, randomised controlled clinical trial," *BMJ Open*, vol. 8, no. 7, Jul. 2018, Art. no. e021039, doi: 10.1136/bmjopen-2017-021039.
[38] S. Damercheli, M. Buist, and M. Ortiz-Catalan, "Mindful sensorimotor therapy combined with brain modulation for the treatment of pain in individuals with disarticulation or nerve injuries: A single-arm clinical trial," *BMJ Open*, vol. 13, no. 1, 2023, Art. no. e059348, doi: 10.1136/bmjopen-2021-059348.
[39] A. M. De Nunzio et al., "Relieving phantom limb pain with multimodal sensory-motor training," *J. Neural Eng.*, vol. 15, no. 6, 2018, Art. no. 066022, doi: 10.1088/1741-2552/aae271.
[40] H. C. Stronks, J. Walker, D. J. Parker, and N. Barnes, "Training improves vibrotactile spatial acuity and intensity discrimination on the lower back using coin motors," *Artif. Organs*, vol. 41, no. 11, pp. 1059–1070, 2017, doi: 10.1111/aor.12882.
[41] L. Sardi, A. Idri, and J. L. Fernández-Alemán, "A systematic review of gamification in e-Health," *J. Biomed. Inform.*, vol. 71, pp. 31–48, 2017, doi: 10.1016/j.jbi.2017.05.011.

Mirka Buist received the B.Sc. degree in industrial design engineering (with the Hons. degree in mathematics) from the University of Twente, Enschede, The Netherlands, in 2019, and the M.Sc. degree in industrial design engineering from the University of Twente, Enschede, The Netherlands, in 2021. She is currently a Research Engineer and Engineering Manager with the Center for Bionics and Pain Research, Sweden.

Shahrzad Damercheli received the B.Sc. degree in mechanical engineering from the University of Tehran, Tehran, Iran, in 2016, and the M.Sc. degree in biomedical engineering in 2021 from the Chalmers University of Technology, Gothenburg, Sweden, where she is currently working toward the Ph.D. degree in electrical engineering. From 2016 to 2019, she was a Research Engineer with the Department of Oral and Maxillofacial Surgeries, Tehran University of Medical Sciences, Tehran, Iran.

Minh Tat Nhat Truong received the B.Sc. degree in control & automation engineering from the Ho Chi Minh City University of Technology, Ho Chi Minh City, Vietnam, in 2017, and the M.Sc. degree in mechanical engineering from Tohoku University, Sendai, Japan, in 2020. From 2020 to 2021, he was a Visiting Researcher with the Center for Bionis and Pain Research, Sweden. He is currently working toward the Ph.D. degree in biomechanics with the KTH Royal Institute of Technology, Stockholm, Sweden.

Alessio Sanna received the B.Sc. degree in biomedical engineering from the University of Cagliari, Cagliari, Italy, in 2020. In 2021, he was a Visiting Researcher with the Center for Bionis and Pain Research, Sweden. He is currently working toward the M.Sc. degree in electronic Engineering with the Politecnico di Torino, Torino, Italy.

Enzo Mastinu received the M.Sc. degree with top grade in electronic engineering from the Università degli Studi di Cagliari, Cagliari, Italy, in 2014, and the Ph.D. degree in biomedical engineering from the Chalmers University of Technology, Sweden, in 2019. He is currently a Marie Skłodowska-Curie Fellow Researcher within the Artificial Hands Area of the BioRobotics Institute, Sant'Anna School of Advanced Studies, Italy. His research focuses on prosthetic control for upper limb amputees and the research interests cover electrical equipment for rehabilitation, embedded systems and electronics design, bioelectric signal acquisition and processing, machine learning and shared-control, and bone-anchored prostheses.

Max Ortiz-Catalan (Senior Member, IEEE) was born in Toluca, Mexico, in 1982. He received the Electronics Engineering degree from ITESM Campus Toluca, Mexico, in 2005, and the M.Sc. degree in complex adaptive systems and the Ph.D. degree in biomedical engineering from the Chalmers University of Technology (CTH), Gothenburg, Sweden, in 2009 and 2014, respectively. He is currently a Full Professor with CTH and Senior Research Scientist with the Bionics Institute, Melbourne, Australia. In 2021, he founded the Center for Bionics and Pain Research (@CBPR.se), where he is the Director. His research interests include bioelectric signals acquisition electronics (analog and digital), signal processing and artificial intelligence algorithms for decoding motor volition and control, neuromuscular interfaces, bone-anchored prostheses and osseointegration, virtual and augmented reality for neuromuscular rehabilitation, and the treatment of neuropathic pain. Dr. Ortiz-Catalan was the recipient of the several honors, notably the European Youth Award in 2014, Delsys Prize in 2016, Brian & Joyce Blatchford Award in 2017, and Swedish Embedded Award in 2018.